

Virtual Screening of PRK1 Inhibitors: Ensemble Docking, Rescoring Using Binding Free Energy Calculation and QSAR Model Development

Inna Slyntko,[†] Michael Scharfe,[†] Tobias Rumpf,[‡] Julia Eib,[‡] Eric Metzger,[§] Roland Schüle,[§] Manfred Jung,[‡] and Wolfgang Sippl*,[†]

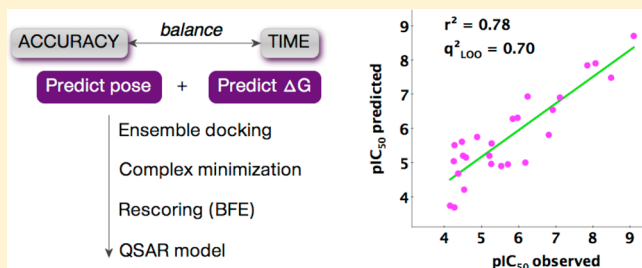
[†]Institute of Pharmacy, MLU Halle-Wittenberg, 06120 Halle (Saale), Germany

[‡]Institute of Pharmaceutical Sciences, University of Freiburg, 79104 Freiburg, Germany

[§]Department of Urology/Women's Hospital and Center for Clinical Research, University of Freiburg Medical Center, 79106 Freiburg, Germany

Supporting Information

ABSTRACT: Protein kinase C Related Kinase 1 (PRK1) has been shown to be involved in the regulation of androgen receptor signaling and has been identified as a novel potential drug target for prostate cancer therapy. Since there is no PRK1 crystal structure available to date, multiple PRK1 homology models were generated in order to address the protein flexibility. An in-house library of compounds tested on PRK1 was docked into the ATP binding site of the generated models. In most cases a correct pose of the inhibitors could be identified by ensemble docking, while there is still a challenge of finding a reasonable scoring function that is able to rank compounds according to their biological activity. We estimated the binding free energy for our data set of structurally diverse PRK1 inhibitors using the MM-PB(GB)SA and QM/MM-GBSA methods. The obtained results demonstrate that a correlation between calculated binding free energies and experimental IC₅₀ values was found to be usually higher than using docking scores. Furthermore, the developed approach was tested on a set of diverse PRK1 inhibitors taken from literature, which resulted in a significant correlation. The developed method is computationally inexpensive and can be applied as a postdocking filter in virtual screening as well as for optimization of PRK1 inhibitors in order to prioritize compounds for further biological characterization.



INTRODUCTION

Phosphorylation of proteins by kinases has been shown to play a significant role in signal transduction cascades by regulating versatile cellular processes such as cell proliferation, differentiation and apoptosis.^{1,2} Kinases transfer the γ-phosphate of adenosine-5'-triphosphate (ATP) to specific amino acids with a free hydroxyl group (serine, threonine, or tyrosine). Deregulation of kinase function or abnormal phosphorylation has been implicated in various pathological conditions such as cancer and infectious diseases as well as in metabolic, immunological, and neurological disorders.^{1–3} Therefore, protein kinases have now become one of the most prospective therapeutic drug targets.

Being one of the largest and diverse protein families, kinases mediate a large number of biological processes. Manning et al. have defined 518 kinases encoded in the human genome.⁴ Despite the remarkable sequence diversity within this enzyme class, they share a universal secondary structure of the catalytic domain. Moreover, the residues within the ATP binding cleft are highly conserved among various kinase families. This makes the search of highly selective ATP-competitive inhibitors challenging. Nevertheless, there are certain differences in

regions adjacent to the binding cleft, which ATP does not occupy. Such less conserved parts of the protein provide an opportunity for the design of selective ATP-competitive inhibitors. Thus, a detailed knowledge of the protein structure is needed to assist the rational design of kinase inhibitors.

Protein kinase C related kinase (PRK1, also known as PKN1) is a serine/threonine kinase and a coactivator of the androgen receptor (AR).⁵ It was shown that PRK1 is implicated in tumorigenesis, and it is considered as a promising therapeutic target for prostate cancer therapy.⁶ However, only little is known about PRK1 inhibitors and the consequences of its inhibition. Therefore, the development of novel specific compounds with significant activity against PRK1 is currently a subject of great interest.

Molecular docking is one of the main techniques used in structure-based drug discovery since it is a fast and simple method.^{7–11} Different studies have shown that docking-based virtual screening (VS) of large compound databases can be applied effectively for the identification of novel hits.^{12–14}

Received: October 28, 2013

Published: December 30, 2013



Despite its great potential, the method has a number of drawbacks and limitations.^{15–17} The two major tasks of molecular docking include the determination of correct ligand orientation within the protein active site and the assessment of protein–ligand affinity. Whereas docking methods already show good results in the prediction of binding modes, the second task still remains a key challenge in computational chemistry. Considering the balance between the accuracy of calculations and the computational cost, scoring functions were developed on the basis of simplified empirical force fields or potentials of mean force using certain approximations, e.g. they usually do not take solvation effects or protein flexibility into account. Thus, accurate prediction of the binding affinity using docking methodologies remains an elusive goal, and there is the need for more precise methods for its evaluation.

Various approaches were developed in order to improve the docking performance, e.g. docking to an ensemble of protein structures, normalizing docking scores, or using rescoring procedures. Different studies have shown that docking methods perform well in reproducing ligand binding poses for experimentally derived structures; however, they can fail if a protein structure was solved in the presence of a very different compound.¹⁸ It is known that during ligand binding conformational changes of a protein can occur. In fact, even small changes in a receptor structure can be important for ligand binding. Thus, using rigid receptor structures can hamper correct ligand docking, for example, the active ligands will not be docked correctly into a receptor or can be scored poorly. One of the approaches, which handle protein flexibility, is the so-called “ensemble docking”.^{19–21} Here, a ligand is docked into several protein structures/conformations in order to identify the best-scored pair of protein conformation and ligand binding mode. In the present work, we used an ensemble of PRK1 homology models refined in the presence of active inhibitors from different chemical classes for docking studies.

Correct ranking of compounds according to their binding affinity is another critical issue. Over the last years a large effort has been undertaken to address this question. The approaches vary from simple methods like rescoring of poses with external scoring functions, consensus scoring, normalization, etc.²² to more sophisticated and power-demanding calculations of binding free energy (BFE) such as linear interaction energy (LIE), molecular mechanic/Poisson–Boltzmann (generalized Born) surface area (MM-PB(GB)SA), free-energy perturbation (FEP), and thermodynamic integration (TI).^{23–26} Although some studies show successful examples of lead optimization using FEP and TI methods, they are still rarely applied in the drug discovery process, mainly due to the high computational costs. Nevertheless, the recent increase in computing power made it possible to apply some BFE calculation methods on quite large compound data sets. This allows using them not only on the late stages of drug discovery but also as a tool for postprocessing of virtual screening results. The number of studies, reporting on the successful application of MM-PBSA, MM-GBSA methods for the estimation of protein–ligand binding affinities, is increasing, and automated procedures for BFE estimation applicable for a large compound selection have been developed.^{27–33}

Traditionally, MM-PB(GB)SA calculations are carried out using a number of snapshots derived from equilibrated molecular dynamics (MD) simulation. Various studies have demonstrated the efficacy of this approach for predicting binding affinities;^{30,31,34,35} however, due to the limitations in

computational power, it is usually applied for a small subset of molecules. Recent publications report that the calculation of BFE using a single snapshot derived from a short complex minimization in implicit solvent, in some cases combined with short molecular dynamics simulation, can also result in a good correlation with experimental data.^{36–40}

Furthermore, the combined quantum mechanics/molecular mechanics (QM/MM) scoring function implemented in AMBER⁴¹ was tested for calculating the binding affinity.^{42,43} This method allows treating a small part of the complex, e.g. the ligand and residues of the active site, with semiempirical QM calculations, while the remaining part is treated by classical molecular mechanics as a fixed charge background. Such a procedure considers electronic effects such as polarization^{44–47} and charge transfer⁴⁸ for the selected part of the complex, which can play an important role in ligand binding to the target and are usually not considered in classical BFE calculations.

Most of the studies using MM-PBSA, MM-GBSA for BFE calculations show good results for congeneric series of compounds in a given receptor or for structurally diverse ligands, but with known binding modes taken from the PDB.^{27,31,49} However, in a VS experiment usually a large set of diverse inhibitors is fitted into the protein structure and the ligand conformation is usually selected according to the best docking score. In the current study, we wanted to test the performance of different BFE calculation methods such as MM-PB(GB)SA, QM/MM-GBSA on their ability to predict the relative binding affinity of structurally different PRK1 inhibitors from in-house and published data sets. Furthermore, we included inactive compounds in our studies in order to see which of the approaches performs best in discrimination. The BFE model showing the best performance in enrichment studies as well as in the prediction of the biological activity represents a valuable tool for optimization of the identified PRK1 inhibitors.

MATERIALS AND METHODS

Homology Modeling. To identify which experimentally known 3D structures can serve as a template to generate a homology model of PRK1, a BLAST search was carried out through the NCBI.⁵⁰ The sequence of human PRK1 kinase domain (UniProt ID Q16512, residues 610–940) was used as query. The structures available in the PDB, showing the highest similarity to the PRK1 sequence, belong to the PKC family. It was revealed that all these structures show the active kinase conformation. Among them, the crystal structure of PKC-theta (PDB code 2JED, resolution 2.32 Å) was chosen as template as it shows the highest sequence identity with PRK1 (50%) and covers 99% of the whole sequence query. The homology model building was carried out using the Modeller 9v8 software.⁵¹

The sequence alignment of PRK1 and PKC-theta (see Figure S1 of the Supporting Information) was made using the default Modeller align2d parameters. On the basis of the PKC-theta template structure and the alignment file, five models of PRK1 were generated. The model with the lowest value of the Modeller objective function or the DOPE assessment score was chosen for further analysis.⁵² Further refinement was proceeded using Protein Preparation Wizard of Schrödinger Suite 2012.⁵³ Hydrogen atoms and partial charges were assigned, and the model was energy minimized applying the OPLS2005 force field.^{54,55} The quality of the model (hm_prk1) was analyzed by means of stereochemical analysis with the PROCHECK program (see Figure S2 of the Supporting Information) and

Protein Report tool implemented in Maestro v9.3.⁵³ The stability of the derived homology model was examined by means of molecular dynamics simulations using AMBER 12.⁵⁶ The RMSD plot showed that the protein backbone atoms remained stable (near 2.5 Å) after the equilibration period (see Figure S3a of the Supporting Information).

Model Refinement. The binding site of the initially generated PRK1 model (hm_prk1) was refined by including structural information about the ligand (i.e., staurosporine) using Modeller 9v8. For this the crystal structure of PKC-theta in complex with staurosporine at 2 Å resolution (PDB code 1XJD) was taken from the PDB. The sequence of PRK1 was aligned to the initial model from the previous step (hm_prk1) and to the edited 1XJD structure containing residues of the binding site. Next, the alignment file and modeling script were modified for including the ligand into the refined homology model. The relative orientation of the ligand and the target was specified by restrained ligand–protein interactions within the binding site (hinge region residue Ser698). The conformation of the ligand was assumed to be rigid. Five models were generated, and the best model was selected according to the lowest DOPE assessment score. Thus, a new homology model of PRK1 (hm_STU) with bound ligand was obtained. In a similar way, the binding site of PRK1 model (hm_prk1) was refined in the presence of other inhibitors (HA-1077, Nvp-Xaa228, CP-690550,⁵⁷ GSK-690693⁵⁷). The choice of the ligands for refinement was based on the structural diversity of the compounds as well as on different binding modes observed for these inhibitors, which could not be reproduced correctly by docking into a single protein structure. Furthermore, the residues 887–940 of the C-terminal loop were included in the model hm_2esm_1, whose structure was refined with the inhibitor HA-1077. In total, six homology models were built. The stability of the models was confirmed through 10 ns of molecular dynamics simulation. All models gave relatively stable trajectories (see Figure S3b–f of the Supporting Information).

Molecular Dynamics Simulations. The MD simulations were carried out using AMBER 12⁵⁶ and the AMBER ff99SB⁵⁸ force field. The explicit solvent model TIP3P was used.⁵⁹ The protein was placed in a box of water molecules with a margin of 10 Å. Four steps of minimization each of 3000 iterations (500 of steepest descent and 2500 of conjugate gradient) were carried out. In the first step, water molecules and ions were minimized while protein atoms were restrained to the initial coordinates with a force constant 10 kcal·mol⁻¹·Å⁻². In the second step, the protein side-chains were minimized together with the solvent (protein backbone was restrained). During the next step, only a weak restraint of 0.01 kcal·mol⁻¹·Å⁻² was applied on the protein backbone. Finally, all restraints were removed and the entire system was minimized.

The temperature of the system was then equilibrated at 300 K through 100 ps of MD using 2 fs time steps. A constant volume periodic boundary was set to equilibrate the temperature of the system by the Langevin dynamics⁶⁰ using a collision frequency of 2 ps⁻¹. During the temperature equilibration routine, the protein in the solvent box was restrained to the initial coordinates with a weak force constant of 10 kcal·mol⁻¹·Å⁻². To avoid inaccurate calculations of pressure, the next 100 ps of MD were run at constant volume. The pressure of the solvated system was equilibrated at 1 bar in constant pressure periodic boundary by an isotropic pressure scaling method with pressure relaxation time of 1 ps.

Before running free MD simulations, the system was slowly equilibrated in four steps (each 100 ps) using constraints like in minimization steps. The time step was set to 2 fs with a cutoff of 9 Å for the nonbonded interaction, and the SHAKE⁶¹ option was employed to keep all bonds involving hydrogen atoms rigid. Electrostatic interactions were computed using the particle mesh Ewald method.⁶² Each MD simulation was performed for 10 ns.

Molecular Docking. All docking calculations were performed using the Glide program implemented in Schrödinger Suite 2012.^{63–66} A hydrogen bond constraint was defined at the hinge residue Ser698. All other parameters for the grid generation were kept as default. The ligands were prepared using LigPrep⁶⁸ within the Schrödinger utility MAESTRO by generation of ionization and tautomeric states at pH 7.4 and with less than 10 low-energy ring conformations. All ligands were energy-minimized using the MMFFs force field implemented in MAESTRO. The Glide standard precision mode (GlideSP) was used for flexible ligand docking. The options were set to penalize nonplanar conformations of amide bonds and to enhance planarity of conjugated pi groups. In order to optimize highly strained ligand geometries, a postdocking minimization including five poses per ligand was applied. Compounds were docked into each of the protein structures and the top-scoring pose for each ligand was kept for further analysis. In case of ensemble docking, the docking results for different homology models were merged and the best solution for each ligand was selected.

MM-PB(GB)SA and QM/MM-GBSA Calculations for Rescoring the Docking Results. The selected top-scored docking solutions for each compound with the corresponding model were subjected to further refinement by means of energy minimization and rescoring using three approaches for BFE calculations, namely MM-PBSA, MM-GBSA, and QM/MM-GBSA.

According to the MM-PB(GB)SA method, the BFE between ligand and receptor (ΔG_{bind}) is computed as a sum of the changes of the gas-phase molecular mechanics energies (ΔE_{MM}), polar and nonpolar solvation energy (ΔG_{solv}), and conformational entropy ($-T\Delta S$) upon binding; see eq 1:^{67,68}

$$\Delta G_{\text{bind}} = \Delta E_{\text{MM}} + \Delta G_{\text{solv}} - T\Delta S \quad (1)$$

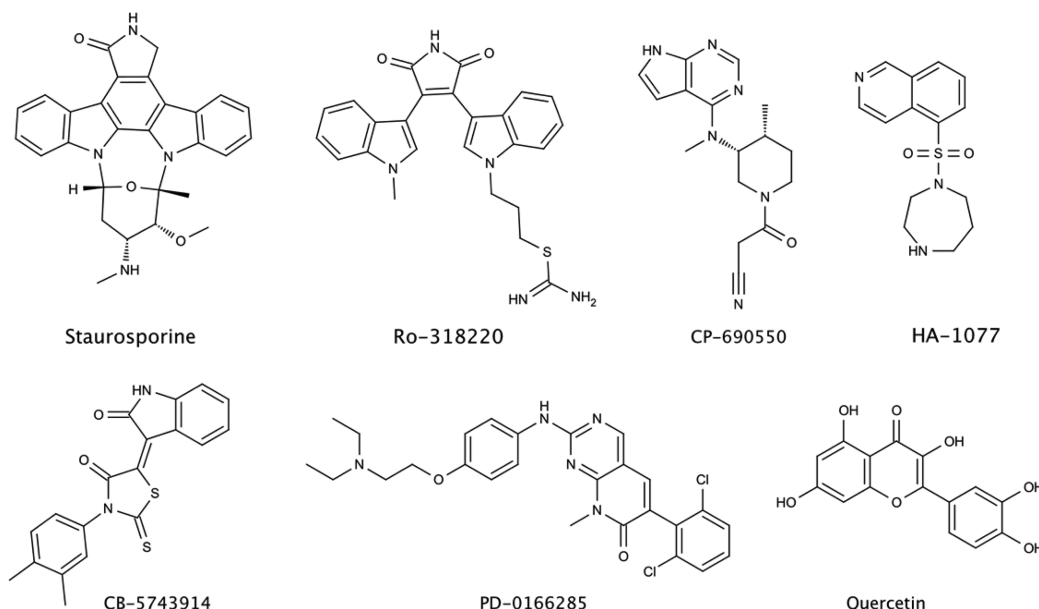
$$\Delta E_{\text{MM}} = \Delta E_{\text{internal}} + \Delta E_{\text{vdW}} + \Delta E_{\text{ele}} \quad (2)$$

$$\Delta G_{\text{solv}} = \Delta G_{\text{PB/GB}} + \Delta G_{\text{SASA}} \quad (3)$$

$$\Delta G_{\text{SASA}} = \gamma \text{SASA} + b \quad (4)$$

Correspondingly, ΔE_{MM} includes differences in bond, angle, dihedral energies ($\Delta E_{\text{internal}}$), van der Waals (ΔE_{vdW}), and electrostatic energies (ΔE_{ele}); see eq 2. The polar solvation contribution is usually computed by solving the generalized Born (GB) or Poisson–Boltzmann (PB) equation, while the nonpolar term is determined as a linear function of the solvent-accessible surface area (SASA);⁶⁹ see eqs 3 and 4. The entropy contribution can be calculated using normal-mode analysis. However, in the practice this term is often neglected for congeneric series.^{31,36,39}

Force field parameters were assigned for ligand and protein using the Leap module in AMBER12.⁵⁶ General Amber force field (GAFF)⁷⁰ and AM1-BCC⁷¹ charges were used for ligands, and the AMBER ff99SB⁵⁸ force field was used for proteins. The minimization of protein–ligand complexes was done in an

**Figure 1.** Representative PRK1 inhibitors from DS1, showing different hinge-binding scaffolds.**Table 1. PRK1 Inhibitors along with Experimental Activity and Standard Error of Mean^a**

name	supplier	IC ₅₀ (PRK1), nM	±SEM, nM	pIC ₅₀	screening ^b
Staurosporine	Biomol	0.8	0.2	9.10	1
K252a	Biomol	3.2	0.6	8.49	1
Lestaurtinib	Biomol	8.6	0.9	8.07	1
PKC-412	Biomol	14.2	1.5	7.85	1
Ro-318220	Biomol	78.3	8.6	7.11	1
CP-690550	Sigma-Aldrich	129	29	6.92	3
BIM IV	Sigma-Aldrich	154.2	49	6.81	3
BIM I	Biomol	579	140	6.24	2
H-7	Biomol	658	456	6.18	2
PZ0151	Sigma-Aldrich	1060	140	5.97	5
Calbiochem681640	Calbiochem	1441	220	5.84	3
HA-1077	Biomol	1945	465	5.71	2
CB-5743914	ChemBridge	2940	420	5.53	6
CB-6046000	ChemBridge	5350	1880	5.27	6
PD-0166285	Tocris	5517	2471	5.26	3
Z1039084878	Enamine	6210	3180	5.21	5
CB-76536004	ChemBridge	13090	2660	4.88	5
Z991906728	Enamine	26400	2770	4.58	5
Ambnee93542761	Ambinter	29330	4110	4.53	4
Z1139202903	Enamine	31470	4590	4.50	5
CB-85384930	ChemBridge	34020	11820	4.47	5
CB-38374289	ChemBridge	42560	11650	4.37	5
Z1129905037	Enamine	53380	5970	4.27	5
F2458-0011	Ambinter	53730	9590	4.27	4
Z1139203558	Enamine	55730	11520	4.25	5
F2457-0067	Ambinter	70300	7340	4.15	4
Quercetin	Biomol	Inhibition >5 μM			3
K252c	Sigma-Aldrich	Inhibition >1 μM			3

^aIC₅₀ values were determined in a PRK1 in vitro assay as described in the Materials and Methods section. ^b(1) Compounds identified by in vitro screening of the Biomol Kinase and Phosphatase inhibitor screening set at 100 nM threshold concentration. (2) Compounds from biomol screening, for which full IC₅₀ measurement was carried out. (3) Other known kinase inhibitors tested in vitro on PRK1. (4) Inhibitors identified by similarity search using isoquinoline derivative H-7. (5) Inhibitors identified by similarity search using CP-690550. (6) Compounds identified by pharmacophore-based virtual screening using PD-0166285 as a query.

implicit solvent. The complex was minimized for 5000 steps of steepest descent and 5000 steps of conjugate gradient algorithm. Next, the binding free energy calculations were

performed. Only one snapshot per complex derived after minimization was used for it. The MMPBSA.py script implemented in AMBER 12 was used for the calculation of

energy components from eqs 1–3. The internal, van der Waals, and electrostatic terms, representing the gas-phase molecular mechanics energies (ΔE_{MM}), were calculated using the SANDER module with 16 Å cutoff for the long-range nonbonded interactions. The polar solvation free energy was computed via implicit solvation models like Poisson–Boltzmann (PB) or generalized Born (GB) applying the following parameters: modified GB model developed by Onufriev et al.⁷² (GBOBC2, $igb = 5$), salt concentration for GB and ionic strength for PB of 0.15 M, internal dielectric constant of 1.0 for solute and 80 for implicit PB solvent, other parameters were kept default. The nonpolar solvation term was determined from the solvent-accessible surface area (SASA) computed via the molsurf routine following eq 4, where γ was set to 0.0072 and constant b to 0 (default values). The QM/MM-GBSA calculations were done analogically to MM-GBSA with only one difference—the QM part was specified for the ligand and was treated with semiempirical method (RM1),⁷³ while the remaining atoms were treated with ff99SB force field. The entropic contribution to binding was not evaluated since it usually gives large error bars and requires long simulation time; thus, it is often considered equivalent if the relative BFE for congeneric ligand series are analyzed.^{74,75}

PRK1 in vitro Assay. Screening was carried out using the LanthaScreen Eu Kinase Binding Assay Kit (Invitrogen) with final assay concentrations of 5 nM for PRK1 (Proquinase, Freiburg), 2 nM LanthaScreen Eu-anti-GST Antibody (Invitrogen) and 10 nM Kinase Tracer 236 (Invitrogen). The assay was performed in 384-well microtiter plates (PerkinElmer, Rodgau) with a final assay volume of 15 µL (1% (v/v) DMSO). Detection was performed with EnVision 2102 Multilabel Reader (PerkinElmer, Rodgau, excitation 340 nm, first emission 665 nm, second emission 615 nm, delay time 100 µs, integration time 200 µs). IC₅₀ values were determined using Graphpad Prism 5.0 (La Jolla, USA).

RESULTS AND DISCUSSION

Studied Data Set. In the current study we used a data set of compounds (DS1) collected from a number of in vitro screenings carried out in our laboratory. Initially, the Biomol Kinase and Phosphatase inhibitor screening set (84 compounds), containing some generic kinase inhibitors was tested at 100 nM threshold concentration.⁷⁶ This screen identified the highly potent PRK1 inhibitors staurosporine, Ro318220, K252a, and lestaurtinib as well as some moderately active inhibitors (e.g., HA-1077, H-7, and BIM I; see Figures 1, S4a and S4b of the Supporting Information). Later on, further in vitro tests identified PRK1 inhibitors showing diverse chemical structures (e.g., PD-0166285 and CP-690550; see Figure 1). With the intention to identify more diverse inhibitors and to increase the range of activity within the data set, several virtual screening campaigns were initiated. Since staurosporine analogs represent a well-studied class of nonselective kinase inhibitors, we decided to focus our attention on compounds with distinct scaffolds and binding modes. Therefore we took the isoquinolines HA-1077 and H-7, the pyrrolopyrimidine CP-690550, and the 8-methylpyrido[2,3-*d*]pyrimidin-7(8H)-one PD-0166285 and carried out similarity and pharmacophore-based virtual screenings (details not shown). The identified hits were docked into the PRK1 homology model (hm_prk1) using GlideSP. The top-ranked binding poses were visually analyzed, and some compounds were purchased and evaluated for PRK1 inhibition. Several of them showed an inhibition in the micromolar range

(e.g., isoquinolines Ambnee93542761, F2458-0011, F2457-0067; pharmacophore hits CB-5743914 and CB-6046000; pyrrolopyrimidines PZ0151, Z1039084878 and others; see Table 1 and Figure S4b–d of the Supporting Information). Nevertheless, this approach was not able to identify highly active inhibitors such as the staurosporine derivatives, showing that a good docking score may be not a sufficient criterion for compound selection.

The virtual screenings and in vitro tests, applied on different stages of the project, expanded our data set to 328 compounds (28 actives and 300 inactives). Among them 26 compounds were shown to inhibit PRK1 with IC₅₀ values in the range of 0.8 nM–70 µM (see Table 1). Additionally, two compounds showed inhibition of PRK1 at 5 µM (quercetin) and 1 µM (K252c). PRK1 inhibitors representing diverse hinge-binding scaffolds are shown in Figure 1. (The structures of all 28 PRK1 inhibitors as well as the full list of 328 compounds from DS1 in SMILES format can be found in the Supporting Information; see Figure S4 and Attachment 1, correspondingly).

PRK1 Homology Modeling. Since the crystal structure of PRK1 is not available, initially, a homology model (hm_prk1) was generated based on the template PKC-theta (PDB code 2JED), which shares high sequence identity with PRK1. However, not all PRK1 inhibitors could be docked into this initial model correctly. Thus, the conformation of residues in the ATP-binding pocket of model hm_prk1 was adjusted to the presence of several structurally different inhibitors. As a template for this refinement, the conformations of binding pocket and ligand were taken from crystal structures of homologous kinases. In this way, six PRK1 homology models were generated for this study (see Table 2 and the Materials

Table 2. Model Names, Binding Pocket Template Structures, and Inhibitors Used for Refinement of the Homology Models^a

model name	crystal structure used for refinement (PDB ID)	binding pocket template	inhibitor
hm_2esm/hm_2esm_1	2ESM	ROCK1	HA-1077
hm_2jed	2JED	PKC-theta	Nvp-Xaa228 (BIM1 analog)
hm_CP	3LXN	TYK2	CP-690550
hm_GSK	3D0E	AKT2	GSK-690693
hm_STU	1XJD	PKC-theta	Staurosporine

^aThe initial model was generated on the basis of PKC-theta as template structure.

and Methods section for details). All models were obtained by refinement of the initial PRK1 homology model (hm_prk1). Using an ensemble of induced fit models increases conformational sampling of the binding site, which leads to improved pose prediction and scoring performance. The superposed structures of the six PRK1 homology models are shown in Figure 2. The models were superimposed by backbone Cα atoms, as shown in Figure 2a, which resulted in RMSD values in the range of 1.26–2.55 Å. The ATP-pocket residues superimposed by all atoms in the binding site are shown in Figure 2b (RMSD in the range of 0.74–2.50 Å). All models share a high similarity of the ATP binding site, and only minor deviations are observed for some side chains and the P-loop.

Due to the flexibility and lack of structural information, the C-terminal loop flanking the ATP-binding pocket (residues

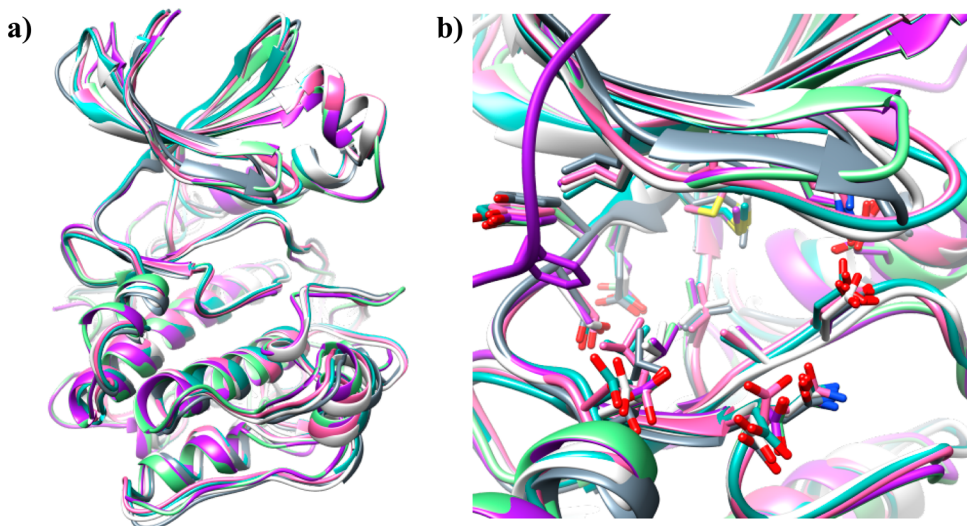


Figure 2. Comparison of the generated PRK1 homology models: (a) structures of six PRK1 homology models, shown as colored ribbons, after superimposition on the backbone C α atoms; (b) conformation of ATP-binding site residues from different PRK1 homology models superimposed by using all pocket residues.

887–940) was not considered in most models except in one (hm_2esm_1). The docking experiments showed that the conformation of this loop could hinder the docking of some inhibitors (e.g., TAE-684, VX-680, or sunitinib). However, the analysis of complexes with isoquinoline derivatives available in PDB showed that a certain conformation of Phe904 of the C-terminal loop (see Figure 3) can play an important role in pose identification and scoring of this type of inhibitors, which is discussed later in this article. In order to take this possibility into account, we decided to keep one model (hm_2esm_1) containing these residues.

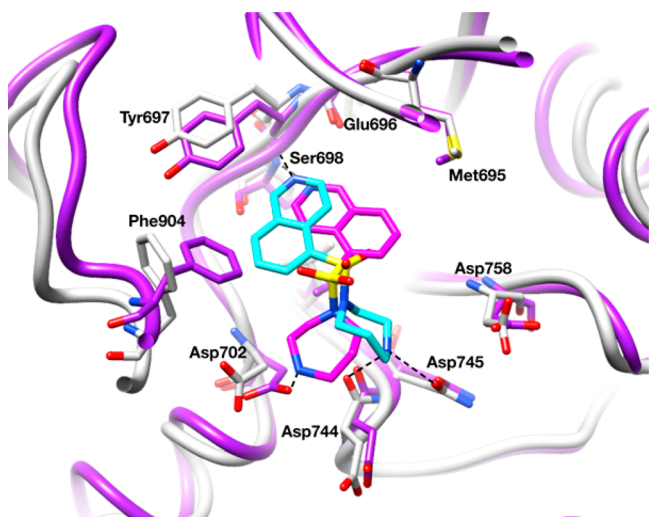


Figure 3. Comparison of the ATP-binding pockets of two PRK1 homology models—hm_STU refined with ligand staurosporine in the binding site (light gray ribbon and sticks; the C-terminal flexible loop, modeled from PKC theta 2JED, is shown in figure for comparison, but it was deleted due to uncertainty in its structure) and hm_2esm_1 refined in the presence of HA-1077 (purple ribbon and sticks). The docking solutions of compound HA-1077 with hm_STU and hm_2esm_1 are shown in cyan and magenta sticks, respectively. Hydrogen bonds between inhibitor and the kinase are displayed as dashed lines.

Docking into a Single Protein Conformation. In the docking studies, we first investigated the performance of each homology model separately. Because there is no experimentally determined structure for PRK1 available, the ability to reproduce the correct docking pose of known inhibitors was evaluated by comparing with binding modes taken from crystal structures of homologous kinases with the same or a closely related inhibitor. The results show that a proper pose can be identified by Glide for a given inhibitor when the correct protein conformation is used. However, the particular model can be limited to the usage for compounds similar to the one used in induced-fit modeling. For example, the side chain of Phe904 within the C-terminal flexible loop is exposed into the ATP-binding pocket in homology model refined for HA-1077 (hm_2esm_1). The phenylalanine makes typical “edge-to-face” aromatic interaction with the ligands HA-1077 and H-1152P in crystal structures with PKA or Rho kinase (PDB structures 1Q8U, 1Q8W, 2ESM, 2GNI) as well as in the homology model of PRK1 with HA-1077. Such a conformation of Phe904 plays an important role in the identification of the correct pose and scoring of compounds similar to HA-1077 during the docking. At the same time, the size of the pocket of hm_2esm_1 is too small to accommodate large ligands like staurosporine and its analogs. Conversely, the homology model refined with staurosporine (hm_STU; see Figure 3) has a larger ATP-binding pocket with Phe904 pointing outside of it; thus, the flipped HA-1077 conformation is usually observed as a result of docking to hm_STU (see Figure 3). The observations clearly show that using only one protein conformation can result in an inaccurate prediction of ligand binding poses and, subsequently, in low enrichment factors, especially when a diverse set of ligands is docked (see Figure 4a). Furthermore, the incorrectness on the stage of docking can mislead further rescoring experiments. It is worth noting that, although some models yield lower enrichment than others, they still can be used in VS or ensemble docking since they can represent a more unique protein conformation that is able to recognize certain types of compounds.

Docking into an Ensemble of PRK1 Conformations. There are several reasons why docking programs fail to identify

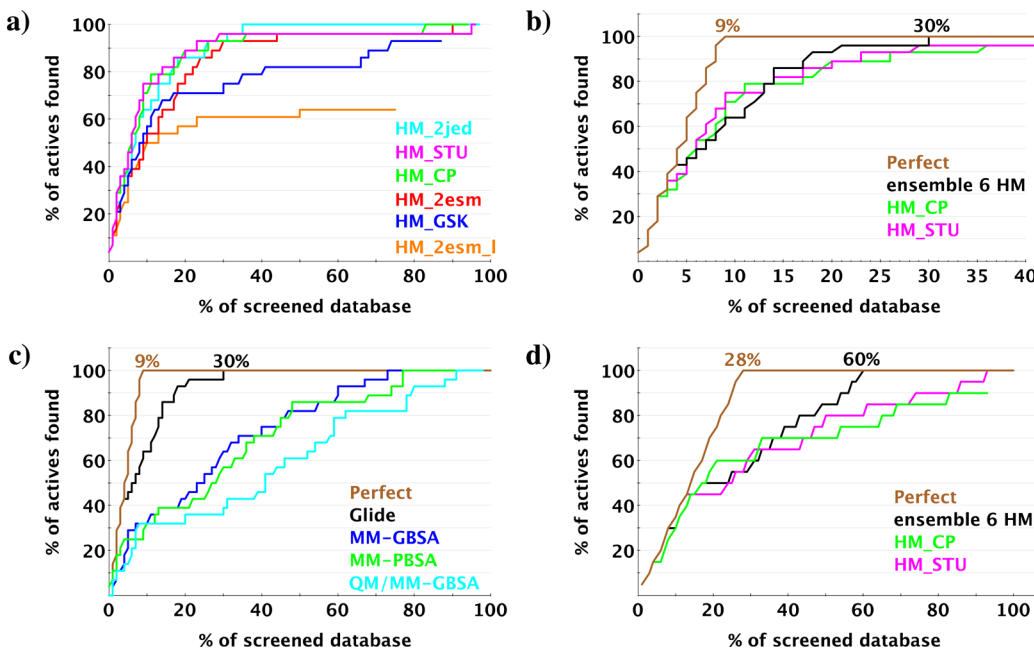


Figure 4. Enrichment plot showing the percentage of actives found at a given percentage of the ranked database for DS1 (a–c) and DS2 (d). The plot compares the performance of the following: (a) docking of DS1 into each single homology model; (b) ensemble docking of DS1 using all six homology models versus the two best single models; (c) ensemble docking of DS1 using different scoring methods—docking score (GlideSP) or BFE scores (MM-PBSA, MM-GBSA, QM/MM-GBSA); (d) ensemble docking of DS2 versus the two best single models. The theoretical perfect curve, when all known PRK1 binders are ranked among the top of database, is shown in brown. In some cases the percentage of active compounds or screened database is not reaching 100%, implicating that Glide did not return poses for some compounds.

the correct ligand pose. Besides the limitations of common scoring functions, the reason may lie in using a wrong protein conformation. The docking methods can fail to recognize an active ligand when some residues in the binding pocket occupy the ligand binding space. To overcome this problem we docked all compounds tested on PRK1 from DS1 in all six PRK1 homology models. An ensemble of protein conformations provides a degree of receptor flexibility, which is often not considered in docking experiments. The optimal docking mode was then selected according to the best GlideSP score. The analysis of ensemble docking results shows an overall improvement in the ranking of active ligands, which are distributed among 30% of the top-ranked compounds in the database (see Figure 4b). In comparison, the best single homology model (hm_2jed) has actives distributed among the top 35% of the database. Even though in this case the difference is not dramatic, it is important that using multiple models leads to better pose prediction for structurally diverse groups of inhibitors. However, if the best performing model for a certain compound class is known, it is computationally favorable to use single receptor docking.

Furthermore, the docking results were evaluated by plotting receiver operating characteristic (ROC) curves, which show the distribution of true positives versus false positives. The corresponding area under the curve (AUC), which describes the quality of enrichment, was calculated. These data are summarized in Figure S5 (see the Supporting Information) illustrating that the ensemble docking approach outperforms single protein models.

Binding Free Energy Calculation for Rescoring of Docking Results. The results of previous VS experiments and biological tests showed that relying only on the docking score might be insufficient for correct ligand scoring according to the biological activity. Even though some of the hits derived from

ligand- and pharmacophore-based screening were active on PRK1, they appeared to be weaker PRK1 inhibitors compared to the corresponding query compounds. The ability to estimate the activity of a compound is one of the critical VS tasks, which aims to reduce the time and costs needed for inhibitor development. Thus, we decided to test the performance of some BFE assessment methods on known PRK1 inhibitors.

DS1, containing 26 active PRK1 inhibitors with available IC₅₀ values, was used for the calculation of binding free energies using a fast postprocessing approach. The top Glide docking solution for each compound in the corresponding homology model was selected and submitted for energy minimization using an implicit solvent model. After this, the binding free energy was evaluated using the MM-PB(GB)SA or QM/MM-GBSA protocol for one snapshot derived after minimization. In order to investigate the performance of different scoring methods on enrichment and correlation with biological activity, the results for different homology models were combined and the best pose of each ligand was selected according to the Glide score.

The enrichment plot shown in Figure 4c indicates that rescoring of poses with MM-PB(GB)SA or QM/MM-GBSA performed worse in the discrimination of active from inactive compounds in comparison to the Glide score. Interestingly, several studies report a better discrimination of known actives from decoys while using MM-PB(GB)SA rescoring methodologies as compared to the AutoDock score.^{30,77} However, the screening performance is usually target- and data set-dependent, which probably can explain success in some cases and failure in others. Nevertheless, the work by Graves et al.⁷⁸ shows contradicting results—rescoring introduces many false positives, especially among the top ranked ligands, as compared to simpler docking protocols. The reason may lie in larger errors when internal energies of the receptor structure are

introduced. Also wrong ligand parametrization or electrostatics treatment might be responsible for larger errors. In addition, minimization of the complex allows the adjustment of the binding site for bigger ligands, including false positives.

Estimating the Biological Activity of PRK1 Inhibitors. We have analyzed the performance of different approaches for their ability to correctly estimate the experimental inhibition data. The results for some single homology models show low correlation with experimental pIC_{50} values (see Table 3),

Table 3. Summary of r^2 Correlation Coefficients for Different Scoring Methods Using Single Homology Models or an Ensemble of Six Homology Models

model name	correlation coefficient (r^2)			
	Glide_SP	MM-GBSA	MM-PBSA	QM/MM-GBSA
hm_2esm_1	(0.51) ^a	0.15	0.02	0.17
hm_2esm	0.18	0.45	0.63	0.59
hm_2jed	0.05	0.29	0.47	0.44
hm_CP	0.32	0.25	0.51	0.40
hm_GSK	0.14	0.39	0.37	0.57
hm_STU	0.30	0.32	0.31	0.54
ensemble	0.42	0.42	0.61	0.53

^aGlide did not return poses for some of compounds.

demonstrating that the protein conformation plays an important role in the ligand pose prediction and BFE calculation. Even though, some improvement of correlation was observed for the models with good enrichment (e.g., hm_2jed and hm_CP), when the rescoring with MM-PBSA was done ($r^2 = 0.47$, RMSE = 1.03, $q_{\text{LOO}}^2 = 0.37$ and $r^2 = 0.51$, RMSE = 0.99, $q_{\text{LOO}}^2 = 0.43$, for hm_2jed and hm_CP, respectively).

Interesting results have been observed for the rescoring of ensemble docking solutions. The best correlation coefficient ($r^2 = 0.61$, RMSE = 0.89, $q_{\text{LOO}}^2 = 0.56$) was obtained when the MM-PBSA method was applied for postprocessing (see Figure 5a). Furthermore, we investigated the effect of other descriptors like ligand charge or number of rotatable bonds on the predicted BFE scores. In order to include the ligand charge we constructed a simple predictive quantitative structure activity relationships (QSAR) model based on two descriptors, namely MM-PBSA score “PBTOT” and ligand charge “FCharge” (QSAR_model_1), using MOE⁷⁹ PLS methodology, which

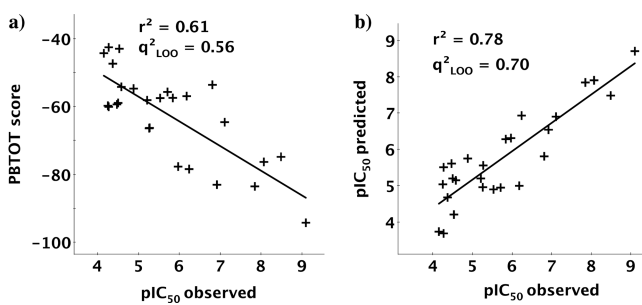


Figure 5. Regression and corresponding correlation coefficients r^2 are shown: (a) between the observed pIC_{50} of 26 PRK1 inhibitors from training set DS1 versus binding free energy scores (PBTOT) calculated by MM-PBSA method using single snapshot after complex minimization; (b) between the observed pIC_{50} versus predicted pIC_{50} by QSAR_model_3 using four descriptors (glideSP-PBTOT-QM/GBTOT-brotN).

resulted in correlation coefficient $r^2 = 0.66$ with root-mean-square error RMSE = 0.82 and cross-validated correlation coefficient $q_{\text{LOO}}^2 = 0.57$. Next, we tested the number of rotatable bonds “brotN” on the QSAR model as descriptor containing information on molecular flexibility and compound’s conformational space.^{80,81} The most interesting results were found when this descriptor was combined with QM/MM-GBSA score “QM/GBTOT” (QSAR_model_2), which led to an improvement of the correlation to $r^2 = 0.68$, RMSE = 0.80, and $q_{\text{LOO}}^2 = 0.61$. Other tested descriptors, such as logP, solvent accessible surface area, or number of heavy atoms, did not improve the quality of the QSAR model (results not shown).

Furthermore, different combinations of descriptors were tested on the model’s predictive power. Finally, the QSAR_model_3 containing four descriptors (MM-PBSA score “PBTOT”, QM/MM-GBSA score “QM/GBTOT”, number of rotatable bonds “brotN”, and Glide score “glideSP_score”) was developed, which resulted in a correlation $r^2 = 0.78$, RMSE = 0.66, $q_{\text{LOO}}^2 = 0.70$ between the predicted and experimental pIC_{50} (Figure 5b). Interestingly, the most potent inhibitors ($\text{IC}_{50} < 100 \text{ nM}$) have a calculated pIC_{50} higher or close to 7, which is in correspondence with the experimental values for these compounds (see Table 4). Thus, the value of

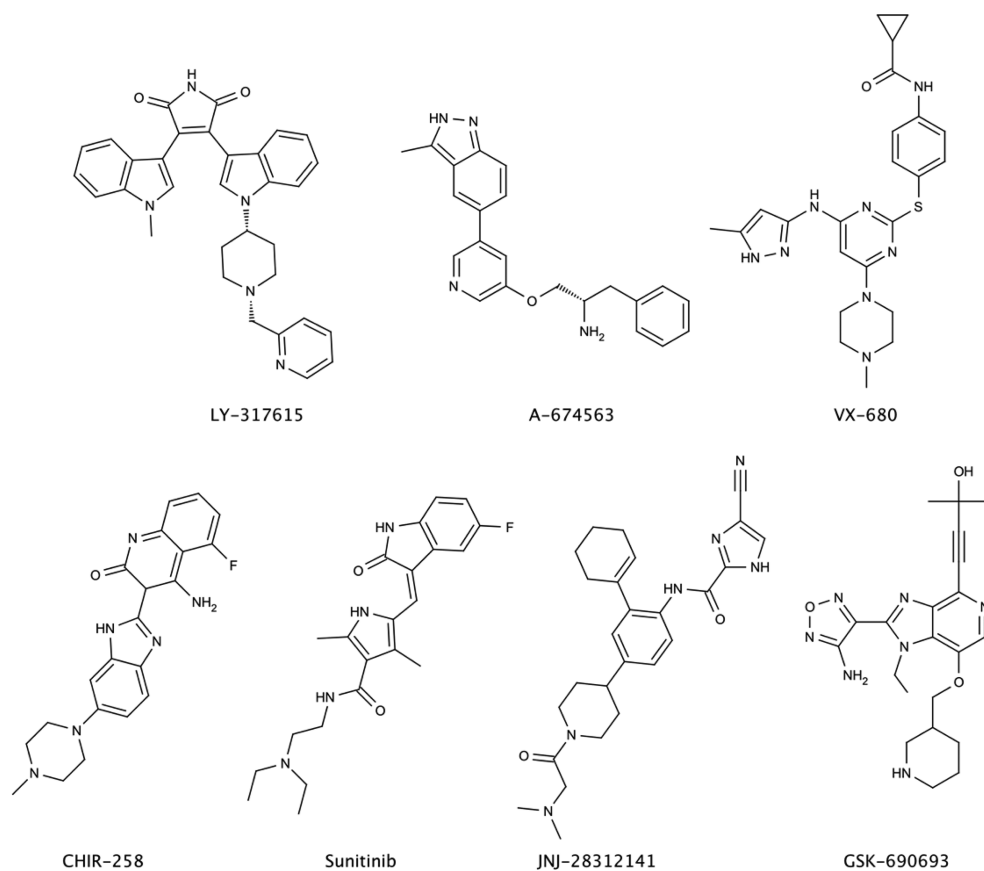
Table 4. Comparison of the Measured pIC_{50} versus the Predicted Values by the QSAR_model_3 for the Most Potent PRK1 Inhibitors from DS1

name	IC_{50} (PRK1), nM	pIC_{50} (PRK1)	predicted pIC_{50} (QSAR_model_3)
Staurosporine	0.8	9.10	8.70
K252a	3.2	8.49	7.48
Lestaurtinib	8.6	8.07	7.90
PKC-412	14.2	7.85	7.84
Ro-318220	78.3	7.11	6.90
CP-690550	120	6.92	6.54

$\text{pIC}_{50} > 7$ could be used as a threshold for the predicted pIC_{50} in order to prioritize compounds for further synthesis or purchase. Such a strategy of rescoring the docking solutions and calculating a predicted pIC_{50} using the developed QSAR model can be especially suitable on the stage of compound optimization, where highly potent inhibitors are of interest.

Validation of the Results. The performance of our protocol for virtual screening and rescoring using MM-PB(GB)SA, QM/MM-GBSA methodologies was further evaluated on an external test data set (DS2) containing 20 diverse PRK1 inhibitors (representative inhibitor structures can be found in Figure 6) and 52 inactive compounds.⁵⁷ Twenty compounds from DS2 were shown to inhibit PRK1 in the range between 1.3 nM and 5 μM (see Table 5). It is worth noting that inhibitors from the second data set are more chemically diverse and have less significant variation in their inhibitory potency in comparison to DS1, which poses a number of challenges in docking and rescoring experiments. The structures of 20 PRK1 inhibitors or 72 compounds from DS2 can be found in Figure S6 or in attachment 1 (as SMILES) of the Supporting Information, correspondingly.

Davis et al. used a different *in vitro* assay for their screening. However, it can be assumed that the inhibitor data of DS1 and DS2 are comparable. This is supported by very similar values obtained for the standard inhibitor staurosporine ($\text{IC}_{50} = 0.8 \pm$

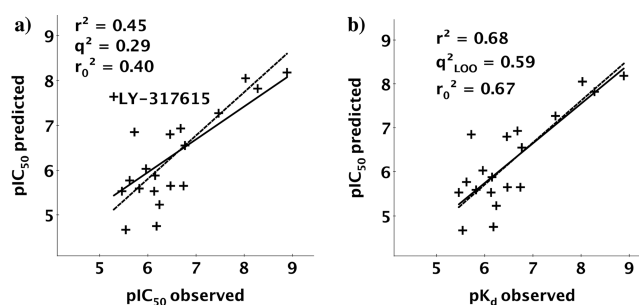
**Figure 6.** Representative subset of PRK1 inhibitors from DS2.**Table 5. Biological Activity of 20 PRK1 Inhibitors Published by Davis et al.⁵⁷**

name	K_d (PRK1), nM	pK_d
staurosporine	1.3	8.89
CEP-701	5.3	8.28
PKC-412	9.3	8.03
GSK-690693	34	7.47
CP-690550	170	6.77
CHIR-258	180	6.74
A-674563	210	6.68
TAE-684	340	6.47
LY-333531	350	6.46
KW-2449	580	6.24
R406	660	6.18
sunitinib	710	6.15
BIBF-1120_deriv	740	6.13
TG-101348	1100	5.96
VX-680	1500	5.82
SU-14813	1900	5.72
JNJ-28312141	2400	5.62
SKI-606	2900	5.54
flavopiridol	3500	5.46
LY-317615	5100	5.29

0.2 nM, $K_d = 1.3$ nM) and PKC-412 ($IC_{50} = 14.2 \pm 2.5$, $K_d = 9.3$ nM). Correspondingly, all compounds of DS2 were docked to all six PRK1 homology models and then the top Glide solutions were rescored using binding free energy calculations after complex minimization. The procedure was done as described above.

Similar to the docking of the first data set, using an ensemble of protein conformations improves the enrichment compared to rigid receptor docking (see Figure 4d) and performs better in identifying a ligand conformation similar to the bioactive one (as compared with known crystal structures).

The correlation between the experimental pIC_{50} and those predicted by the developed QSAR_model_3 was only moderate ($r^2 = 0.45$, $RMSE = 0.71$, $q^2_{LOO} = 0.29$, $r_0^2 = 0.40$), nevertheless, some trends could be observed (see Figure 7a). Therefore, we analyzed the model for outliers, which were detected by large Z-scores. The Z-score represents the absolute difference between the predicted value of the model and the observed biological activity divided by the square root of the

**Figure 7.** Regression between the observed pK_d of PRK1 inhibitors from the test set DS2 versus predicted pIC_{50} by QSAR_model_3: (a) using the data of all 20 active compounds; (b) after removing the outlier (compound LY-317615). The optimal regression line of the model is shown as solid black line, and the regression through the origin of the coordinate system is shown as a dashed black line.

mean square error of the data set. The Z-scores were calculated using the QSAR module of MOE. A compound was considered an outlier if the Z-score was higher than 2.5. Only one outlier was identified, namely compound LY-317615. The comparison of structures of PRK1 with the inhibitor LY-317615 before and after minimization shows that the refining of the complex led to conformational changes within the protein–inhibitor complex, which resulted in a strong interaction pattern between ligand and receptor (Figure 8). This could in part explain the highly

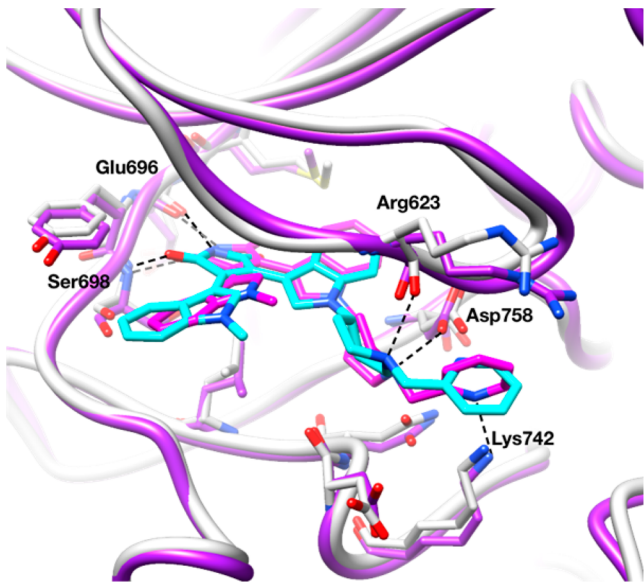


Figure 8. Conformations of compound LY-317615 before (light gray protein and cyan ligand) and after (purple protein and magenta ligand) minimization of the complex along with interacting residues of the binding site are shown. Hydrogen bonds between the inhibitor and the kinase are displayed as dashed lines.

favorable scores for this compound. However, LY-317615 inhibits PRK1 with $K_d = 5100$ nM, and it represents the least potent inhibitor in DS2, suggesting that the binding mode of this compound could be incorrectly predicted or other factors could play a role during the ligand binding, e.g. entropy changes or presence of water in the binding pocket.

Removal of compound LY-317615 improved the results—the correlation coefficient r^2 became equal to 0.68 and the cross-validation correlation coefficient q_{LOO}^2 was 0.59 (see Figure 7b), which is slightly lower than for the validation set. The removal of three duplicates from DS2 (staurosporine, PKC-412, and CP-690550) resulted in correlation $r^2 = 0.49$, RMSE = 0.51, and $q_{\text{LOO}}^2 = 0.26$. It is worth noting that DS2 has a more narrow range of activities (1.3 nM–5 μ M) in comparison to DS1 (0.8 nM–70 μ M), which may be one possible reason for the weaker statistical data. As the results indicate, the MM-PB(GB)SA, QM/MM-GBSA rescoring approach is not accurate enough to distinguish the compounds with similar binding affinities, but it can be used to separate strong PRK1 inhibitors from moderate or weak binders.

Since the data of DS1 and DS2 were obtained in different assays and reported K_d values of DS2 can differ from IC_{50} values of DS1, we additionally generated a QSAR model for DS2. Correspondingly, the same methodology and descriptors were used as for DS1 (QSAR_model_3, MM-PBSA and QM/MM-GBSA scores, number of rotatable bonds, and Glide score). The resulting QSAR model showed slightly different

coefficients for the individual descriptors. This resulted in a correlation coefficient of $r^2 = 0.53$, RMSE = 0.66, and $q_{\text{LOO}}^2 = 0.12$ for the 20 compounds of DS2 with reported activities. After the removal of one outlier (LY-317615, same outlier as observed in the prediction), the correlation was improved to $r^2 = 0.73$, RMSE = 0.49, and $q_{\text{LOO}}^2 = 0.53$ (data not shown).

Furthermore, the predictive ability of the QSAR_model_3 was tested using Golbraikh–Tropsha criteria.^{82–84} They consider that a model with good predictive power should satisfy the following conditions:

- (1) squared correlation coefficient between predicted and observed activities $r^2 > 0.6$;
- (2) squared cross-validation correlation coefficient $q^2 > 0.5$;
- (3) one of the coefficients of determination for regressions through the origin (either predicted vs observed activities r_0^2 or observed vs predicted activities r'_0^2) should have value close to r^2
- (4) $(r^2 - r_0^2)/r^2$ or $(r^2 - r'_0^2)/r^2 < 0.1$ and $0.85 < k$ or $k' > 1.15$, where k and k' are slopes of the regression line through the origin.

The calculated parameters for the test data set and the satisfactory conditions are summarized in Table 6, indicating that the derived model has a good predictive power.

Table 6. Results of the Validation of QSAR_model_3 on the Test Set DS2^a

criteria	calculated value	satisfactory value
r^2	0.677	>0.6
q_{LOO}^2	0.586	>0.5
r_0^2	0.675	$(r_0^2 \text{ or } r'_0^2) \approx r^2$
r'_0^2	0.574	
k	0.952	$0.85 \leq (k \text{ or } k') \geq 1.15$
k'	1.042	
$ r_0^2 - r'_0^2 $	0.101	<0.3
$(r^2 - r_0^2)/r^2$	0.003	
$(r^2 - r'_0^2)/r^2$	0.152	one of these criteria <0.1

^aGolbraikh–Tropsha criteria were used.

Notably, the obtained data show that the most potent inhibitors ($K_d < 100$ nM) from DS2 have a predicted pIC_{50} more than 7 (see Table 7), which is in accordance with the

Table 7. Comparison of Measured Data versus Predicted pIC_{50} by QSAR_model_3 for the Most Potent PRK1 Inhibitors from DS2

name	K_d (PRK1), nM	$\text{p}K_d$ (PRK1)	pIC_{50} predicted (QSAR_model_3)
staurosporine	1.30	8.89	8.18
CEP-701	5.30	8.28	7.82
PKC-412	9.30	8.03	8.05
GSK-690693	34.00	7.47	7.27
CP-690550	170.00	6.77	6.55

results for DS1. These observations demonstrate that the model can be used for the prediction of biological activity and especially for the design of highly potent inhibitors.

CONCLUSION

In the present study, we investigated the performance of docking as well as rescoring using MM-PB(GB)SA, QM/MM-GBSA approaches on two sets of diverse PRK1 inhibitors.

Despite the profound effect of PRK1 on the propagation of androgen receptor driven cancer cell proliferation, there is little information available about the PRK1 structure and its inhibitors. Thus, first we developed a homology model of this enzyme. Next, multiple protein models based on inhibitor-bound conformational states of PRK1 were introduced in order to address protein flexibility. The results show improved docking performance in pose prediction and enrichment when an ensemble of protein conformations is used.

Another question we addressed in this work was the prediction of biological activity. The initial model based only on the docking scores could not explain the activity of compounds as shown by the results of our previous ligand-based or pharmacophore-based VS. The compounds, which were selected on the basis of favorable docking scores, were shown to be only moderately active. Thus, there is need of more sophisticated methods able to evaluate activity of compounds.

The approach presented here employs the estimation of binding free energy using MM-PBSA, MM-GBSA, and QM/MM-GBSA calculations after short minimization of protein-ligand complex using an implicit solvent model. The result demonstrate that using only one snapshot derived after the minimization is sufficient to provide a reasonable prediction of the binding free energy, but only if the correct starting conformation is used. Therefore, in the absence of crystal structures, docking to ensemble of homology models can increase the chance to obtain the correct pose for the ligands. We observed that a significant correlation between calculated relative binding free energies by MM-PBSA method or predicted pIC_{50} by developed QSAR models and experimental IC_{50} values for PRK1 inhibitors can be obtained ($r^2 = 0.61$ using MM-PBSA approach and $r^2 = 0.78$ using QSAR_model_3 on the training set). The results of the validation on the test data set, containing diverse PRK1 inhibitors with reported K_d values, confirmed the good predictive ability of the final QSAR model ($r^2 = 0.68$, $q^2 = 0.59$, $r_0^2 = 0.67$ using QSAR_model_3, one outlier). Furthermore, the approach was able to distinguish potent PRK1 inhibitors ($\text{IC}_{50} < 100 \text{ nM}$) from moderate/weak binders ($\text{IC}_{50} > 100 \text{ nM}$). Nevertheless, despite the good results in predicting the biological activities of known PRK1 inhibitors, the above-described rescore methodology has the disadvantage of weaker discriminating power between active and inactive compounds if compared to the GlideSP score. Thus, the suggested virtual screening strategy for the search of potential PRK1 inhibitors should comprise a combination of ensemble docking methodology with subsequent rescore of the preselected best-scored compounds from the previous step. Furthermore, the compiled in house library of 28 PRK1 inhibitors and 300 true decoys together with the developed approach for predicting the biological activity could be especially useful in the further optimization step of PRK1 kinase inhibitors.

ASSOCIATED CONTENT

Supporting Information

Information regarding PRK1 inhibitors, details of homology modeling such as alignment of PRK1 and PKC-theta sequences and stereochemical analysis of initial PRK1 homology model, RMSD plots for molecular dynamics simulations of different PRK1 homology models as well as ROC curves. This material is available free of charge via the Internet at <http://pubs.acs.org>.

AUTHOR INFORMATION

Corresponding Author

*Phone: +49-345-55-25040. Fax: +49-345-55-27355. E-mail: wolfgang.sippl@pharmazie.uni-halle.de.

Notes

The authors declare no competing financial interest.

ACKNOWLEDGMENTS

This work was supported by the European Regional Development Fund of the European Commission (I.S. and W.S.).

M.J. and R.S. thank the Deutsche Forschungsgemeinschaft for funding (CRC992 Medical Epigenetics—MEDEP).

ABBREVIATIONS

PRK1, Protein kinase C Related Kinase 1; ATP, adenosine-5'-triphosphate; AR, androgen receptor; VS, virtual screening; BFE, binding free energy; LIE, liner interaction energy; MM-PB(GB)SA, molecular mechanic/Poisson–Boltzmann (generalized Born) surface area; FEP, free-energy perturbation; TI, thermodynamic integration; SASA, solvent-accessible surface area; MD, molecular dynamics; MM, molecular mechanics; QM, quantum mechanics; PDB, protein data bank; RMSD, root-mean-square deviation; ROC, receiver operating characteristic; AUC, area under the curve; QSAR, quantitative structure activity relationships

REFERENCES

- Cheetham, G. M. T. Novel Protein Kinases and Molecular Mechanisms of Autoinhibition. *Curr. Opin. Struct. Biol.* **2004**, *14*, 700–705.
- Kondapalli, L.; Soltani, K.; Lacouture, M. E. The Promise of Molecular Targeted Therapies: Protein Kinase Inhibitors in the Treatment of Cutaneous Malignancies. *J. Am. Acad. Dermatol.* **2005**, *53*, 291–302.
- Cohen, P. Protein Kinases — the Major Drug Targets of the Twenty-first Century? *Nat. Rev. Drug Discov.* **2002**, *1*, 309–315.
- Manning, G.; Whyte, D. B.; Martinez, R.; Hunter, T.; Sudarsanam, S. The Protein Kinase Complement of the Human Genome. *Science* **2002**, *298*, 1912–1934.
- Metzger, E.; Yin, N.; Wissmann, M.; Kunowska, N.; Fischer, K.; Friedrichs, N.; Patnaik, D.; Higgins, J. M. G.; Potier, N.; Scheidtmann, K.-H.; et al. Phosphorylation of Histone H3 at Threonine 11 Establishes a Novel Chromatin Mark for Transcriptional Regulation. *Nat. Cell Biol.* **2008**, *10*, 53–60.
- Metzger, E.; Müller, J. M.; Ferrari, S.; Buettner, R.; Schüle, R. A Novel Inducible Transactivation Domain in the Androgen Receptor: Implications for PRK in Prostate Cancer. *Embo J.* **2003**, *22*, 270–280.
- Leach, A. R.; Shoichet, B. K.; Peishoff, C. E. Prediction of Protein-ligand Interactions. Docking and Scoring: Successes and Gaps. *J. Med. Chem.* **2006**, *49*, 5851–5855.
- Yuriev, E.; Ramsland, P. A. Latest Developments in Molecular Docking: 2010–2011 in Review. *J. Mol. Recognit. Jmr* **2013**, *26*, 215–239.
- Cross, J. B.; Thompson, D. C.; Rai, B. K.; Baber, J. C.; Fan, K. Y.; Hu, Y.; Humblet, C. Comparison of Several Molecular Docking Programs: Pose Prediction and Virtual Screening Accuracy. *J. Chem. Inf. Model.* **2009**, *49*, 1455–1474.
- Meng, X.-Y.; Zhang, H.-X.; Mezei, M.; Cui, M. Molecular Docking: A Powerful Approach for Structure-based Drug Discovery. *Curr. Comput. Aided Drug Des.* **2011**, *7*, 146–157.
- Klebe, G. Virtual Ligand Screening: Strategies, Perspectives and Limitations. *Drug Discov. Today* **2006**, *11*, 580–594.
- Kubinyi, H. Success Stories of Computer-Aided Design. In *Computer Applications in Pharmaceutical Research and Development*;

- Ekins, S., Ed.; John Wiley & Sons, Inc.: Hoboken, NJ, 2006; pp 377–424.
- (13) Matter, H.; Sottriffer, C. Applications and Success Stories in Virtual Screening. In *Methods and Principles in Medicinal Chemistry*; Sottriffer, C., Ed.; Wiley-VCH Verlag GmbH & Co. KGaA: Weinheim, Germany, 2011; pp 319–358.
- (14) Seifert, M. H. J.; Lang, M. Essential Factors for Successful Virtual Screening. *Mini Rev. Med. Chem.* **2008**, *8*, 63–72.
- (15) Warren, G. L.; Andrews, C. W.; Capelli, A.-M.; Clarke, B.; LaLonde, J.; Lambert, M. H.; Lindvall, M.; Nevins, N.; Semus, S. F.; Senger, S.; et al. A Critical Assessment of Docking Programs and Scoring Functions. *J. Med. Chem.* **2006**, *49*, 5912–5931.
- (16) Yuriev, E.; Agostino, M.; Ramsland, P. A. Challenges and Advances in Computational Docking: 2009 in Review. *J. Mol. Recognit. Jmr* **2011**, *24*, 149–164.
- (17) Scior, T.; Bender, A.; Tresadern, G.; Medina-Franco, J. L.; Martínez-Mayorga, K.; Langer, T.; Cuanalo-Contreras, K.; Agrafiotis, D. K. Recognizing Pitfalls in Virtual Screening: A Critical Review. *J. Chem. Inf. Model.* **2012**, *52*, 867–881.
- (18) Erickson, J. A.; Jalaie, M.; Robertson, D. H.; Lewis, R. A.; Vieth, M. Lessons in Molecular Recognition: The Effects of Ligand and Protein Flexibility on Molecular Docking Accuracy. *J. Med. Chem.* **2004**, *47*, 45–55.
- (19) McCammon, J. A. Target Flexibility in Molecular Recognition. *Biochim. Biophys. Acta* **2005**, *1754*, 221–224.
- (20) Bolstad, E. S. D.; Anderson, A. C. In Pursuit of Virtual Lead Optimization: The Role of the Receptor Structure and Ensembles in Accurate Docking. *Proteins* **2008**, *73*, 566–580.
- (21) Lin, J.-H.; Perryman, A. L.; Schames, J. R.; McCammon, J. A. The Relaxed Complex Method: Accommodating Receptor Flexibility for Drug Design with an Improved Scoring Scheme. *Biopolymers* **2003**, *68*, 47–62.
- (22) Zhong, S.; Zhang, Y.; Xiu, Z. Rescoring Ligand Docking Poses. *Curr. Opin. Drug Discov. Devel.* **2010**, *13*, 326–334.
- (23) Wang, J.; Morin, P.; Wang, W.; Kollman, P. A. Use of MM-PBSA in Reproducing the Binding Free Energies to HIV-1 RT of TIBO Derivatives and Predicting the Binding Mode to HIV-1 RT of Efavirenz by Docking and MM-PBSA. *J. Am. Chem. Soc.* **2001**, *123*, 5221–5230.
- (24) Gilson, M. K.; Zhou, H.-X. Calculation of Protein-ligand Binding Affinities. *Annu. Rev. Biophys. Biomol. Struct.* **2007**, *36*, 21–42.
- (25) Mobley, D. L.; Dill, K. A. Binding of Small-molecule Ligands to Proteins: “What You See” Is Not Always “What You Get. *Struct. Lond. Engl. 1993* **2009**, *17*, 489–498.
- (26) Michel, J.; Essex, J. W. Prediction of Protein-ligand Binding Affinity by Free Energy Simulations: Assumptions, Pitfalls and Expectations. *J. Comput. Aided Mol. Des.* **2010**, *24*, 639–658.
- (27) Greenidge, P. A.; Kramer, C.; Mozziconacci, J.-C.; Wolf, R. M. MM/GBSA Binding Energy Prediction on the PDBbind Data Set: Successes, Failures, and Directions for Further Improvement. *J. Chem. Inf. Model.* **2013**, *53*, 201–209.
- (28) Homeyer, N.; Gohlke, H. EW: A Workflow Tool for Free Energy Calculations of Ligand Binding. *J. Comput. Chem.* **2013**, *34*, 965–973.
- (29) Parenti, M. D.; Rastelli, G. Advances and Applications of Binding Affinity Prediction Methods in Drug Discovery. *Biotechnol. Adv.* **2012**, *30*, 244–250.
- (30) Rastelli, G.; Del Rio, A.; Degliesposti, G.; Sgobba, M. Fast and Accurate Predictions of Binding Free Energies Using MM-PBSA and MM-GBSA. *J. Comput. Chem.* **2010**, *31*, 797–810.
- (31) Hou, T.; Wang, J.; Li, Y.; Wang, W. Assessing the Performance of the MM/PBSA and MM/GBSA Methods. I. The Accuracy of Binding Free Energy Calculations Based on Molecular Dynamics Simulations. *J. Chem. Inf. Model.* **2011**, *51*, 69–82.
- (32) Uciechowska, U.; Schemies, J.; Scharfe, M.; Lawson, M.; Wichapong, K.; Jung, M.; Sippl, W. Binding Free Energy Calculations and Biological Testing of Novel Thiobarbiturates as Inhibitors of the Human NAD⁺ Dependent Histone Deacetylase Sirt2. *MedChem-Comm* **2012**, *3*, 167.
- (33) Wichapong, K.; Lawson, M.; Pianwanit, S.; Kokpol, S.; Sippl, W. Postprocessing of Protein–Ligand Docking Poses Using Linear Response MM-PBSA: Application to Wee1 Kinase Inhibitors. *J. Chem. Inf. Model.* **2010**, *50*, 1574–1588.
- (34) Ferrari, A. M.; Degliesposti, G.; Sgobba, M.; Rastelli, G. Validation of an Automated Procedure for the Prediction of Relative Free Energies of Binding on a Set of Aldose Reductase Inhibitors. *Bioorg. Med. Chem.* **2007**, *15*, 7865–7877.
- (35) Kuhn, B.; Gerber, P.; Schulz-Gasch, T.; Stahl, M. Validation and Use of the MM-PBSA Approach for Drug Discovery. *J. Med. Chem.* **2005**, *48*, 4040–4048.
- (36) Hou, T.; Wang, J.; Li, Y.; Wang, W. Assessing the Performance of the Molecular mechanics/Poisson Boltzmann Surface Area and Molecular Mechanics/generalized Born Surface Area Methods. II. The Accuracy of Ranking Poses Generated from Docking. *J. Comput. Chem.* **2011**, *32*, 866–877.
- (37) Lindström, A.; Edvinsson, L.; Johansson, A.; Andersson, C. D.; Andersson, I. E.; Raubacher, F.; Linusson, A. Postprocessing of Docked Protein-ligand Complexes Using Implicit Solvation Models. *J. Chem. Inf. Model.* **2011**, *51*, 267–282.
- (38) Lyne, P. D.; Lamb, M. L.; Saeh, J. C. Accurate Prediction of the Relative Potencies of Members of a Series of Kinase Inhibitors Using Molecular Docking and MM-GBSA Scoring. *J. Med. Chem.* **2006**, *49*, 4805–4808.
- (39) Rastelli, G.; Degliesposti, G.; Del Rio, A.; Sgobba, M. Binding Estimation after Refinement, a New Automated Procedure for the Refinement and Rescoring of Docked Ligands in Virtual Screening. *Chem. Biol. Drug Des.* **2009**, *73*, 283–286.
- (40) Sgobba, M.; Caporuscio, F.; Anighoro, A.; Portioli, C.; Rastelli, G. Application of a Post-docking Procedure Based on MM-PBSA and MM-GBSA on Single and Multiple Protein Conformations. *Eur. J. Med. Chem.* **2012**, *58*, 431–440.
- (41) Case, D.; Darden, T.; Cheatham, T.; Simmerling, C.; Wang, J.; Duke, R.; Luo, R.; Walker, R.; Zhang, W.; Merz, K.; et al. *Amber 11*; University of California, San Francisco, 2010.
- (42) Gleeson, M. P.; Gleeson, D. QM/MM as a Tool in Fragment Based Drug Discovery. A Cross-docking, Rescoring Study of Kinase Inhibitors. *J. Chem. Inf. Model.* **2009**, *49*, 1437–1448.
- (43) Hayik, S. A.; Dunbrack, R., Jr.; Merz, K. M., Jr. A Mixed QM/MM Scoring Function to Predict Protein-Ligand Binding Affinity. *J. Chem. Theory Comput.* **2010**, *6*, 3079–3091.
- (44) Illingworth, C. J. R.; Morris, G. M.; Parkes, K. E. B.; Snell, C. R.; Reynolds, C. A. Assessing the Role of Polarization in Docking. *J. Phys. Chem. A* **2008**, *112*, 12157–12163.
- (45) Cho, A. E.; Guallar, V.; Berne, B. J.; Friesner, R. Importance of Accurate Charges in Molecular Docking: Quantum Mechanical/molecular Mechanical (QM/MM) Approach. *J. Comput. Chem.* **2005**, *26*, 915–931.
- (46) Garcia-Viloca, M.; Truhlar, D. G.; Gao, J. Importance of Substrate and Cofactor Polarization in the Active Site of Dihydrofolate Reductase. *J. Mol. Biol.* **2003**, *327*, 549–560.
- (47) Ji, C. G.; Zhang, J. Z. H. Protein Polarization Is Critical to Stabilizing AF-2 and Helix-2' Domains in Ligand Binding to PPAR-gamma. *J. Am. Chem. Soc.* **2008**, *130*, 17129–17133.
- (48) Raha, K.; Peters, M. B.; Wang, B.; Yu, N.; Wollacott, A. M.; Westerhoff, L. M.; Merz, K. M., Jr. The Role of Quantum Mechanics in Structure-based Drug Design. *Drug Discov. Today* **2007**, *12*, 725–731.
- (49) Del Rio, A.; Baldi, B. F.; Rastelli, G. Activity Prediction and Structural Insights of Extracellular Signal-regulated Kinase 2 Inhibitors with Molecular Dynamics Simulations. *Chem. Biol. Drug Des.* **2009**, *74*, 630–635.
- (50) Altschul, S. F.; Gish, W.; Miller, W.; Myers, E. W.; Lipman, D. J. Basic Local Alignment Search Tool. *J. Mol. Biol.* **1990**, *215*, 403–410.
- (51) Sali, A.; Blundell, T. L. Comparative Protein Modelling by Satisfaction of Spatial Restraints. *J. Mol. Biol.* **1993**, *234*, 779–815.
- (52) Shen, M.-Y.; Sali, A. Statistical Potential for Assessment and Prediction of Protein Structures. *Protein Sci. Publ. Protein Soc.* **2006**, *15*, 2507–2524.

- (53) Maestro, Version 9.3; Schrödinger, LLC: New York, 2012.
- (54) Jorgensen, W. L.; Maxwell, D. S.; Tirado-Rives, J. Development and Testing of the OPLS All-Atom Force Field on Conformational Energetics and Properties of Organic Liquids. *J. Am. Chem. Soc.* **1996**, *118*, 11225–11236.
- (55) Shivakumar, D.; Williams, J.; Wu, Y.; Damm, W.; Shelley, J.; Sherman, W. Prediction of Absolute Solvation Free Energies Using Molecular Dynamics Free Energy Perturbation and the OPLS Force Field. *J. Chem. Theory Comput.* **2010**, *6*, 1509–1519.
- (56) Case, D. A.; Darden, T. A.; Cheatham, III, T. E.; Simmerling, C. L.; Wang, J.; Duke, R. E.; Luo, R.; Walker, R. C.; Zhang, W.; Merz, K. M.; et al. AMBER 12; University of California, San Francisco, 2012.
- (57) Davis, M. I.; Hunt, J. P.; Herrgard, S.; Ciceri, P.; Wodicka, L. M.; Pallares, G.; Hocker, M.; Treiber, D. K.; Zarrinkar, P. P. Comprehensive Analysis of Kinase Inhibitor Selectivity. *Nat. Biotechnol.* **2011**, *29*, 1046–1051.
- (58) Hornak, V.; Abel, R.; Okur, A.; Strockbine, B.; Roitberg, A.; Simmerling, C. Comparison of Multiple Amber Force Fields and Development of Improved Protein Backbone Parameters. *Proteins* **2006**, *65*, 712–725.
- (59) Jorgensen, W. L.; Chandrasekhar, J.; Madura, J. D.; Impey, R. W.; Klein, M. L. Comparison of Simple Potential Functions for Simulating Liquid Water. *J. Chem. Phys.* **1983**, *79*, 926.
- (60) Pastor, R. W.; Brooks, B. R.; Szabo, A. An Analysis of the Accuracy of Langevin and Molecular Dynamics Algorithms. *Mol. Phys.* **1988**, *65*, 1409–1419.
- (61) Ryckaert, J.-P.; Ciccotti, G.; Berendsen, H. J. . Numerical Integration of the Cartesian Equations of Motion of a System with Constraints: Molecular Dynamics of N-alkanes. *J. Comput. Phys.* **1977**, *23*, 327–341.
- (62) Darden, T.; York, D.; Pedersen, L. Particle Mesh Ewald: An N-log(N) Method for Ewald Sums in Large Systems. *J. Chem. Phys.* **1993**, *98*, 10089.
- (63) Glide, Version 5.8; Schrödinger, LLC: New York, 2012.
- (64) Friesner, R. A.; Banks, J. L.; Murphy, R. B.; Halgren, T. A.; Klicic, J. J.; Mainz, D. T.; Repasky, M. P.; Knoll, E. H.; Shelley, M.; Perry, J. K.; et al. Glide: a New Approach for Rapid, Accurate Docking and Scoring. 1. Method and Assessment of Docking Accuracy. *J. Med. Chem.* **2004**, *47*, 1739–1749.
- (65) Friesner, R. A.; Murphy, R. B.; Repasky, M. P.; Frye, L. L.; Greenwood, J. R.; Halgren, T. A.; Sanschagrin, P. C.; Mainz, D. T. Extra Precision Glide: Docking and Scoring Incorporating a Model of Hydrophobic Enclosure for Protein-ligand Complexes. *J. Med. Chem.* **2006**, *49*, 6177–6196.
- (66) Halgren, T. A.; Murphy, R. B.; Friesner, R. A.; Beard, H. S.; Frye, L. L.; Pollard, W. T.; Banks, J. L. Glide: a New Approach for Rapid, Accurate Docking and Scoring. 2. Enrichment Factors in Database Screening. *J. Med. Chem.* **2004**, *47*, 1750–1759.
- (67) Kollman, P. A.; Massova, I.; Reyes, C.; Kuhn, B.; Huo, S.; Chong, L.; Lee, M.; Lee, T.; Duan, Y.; Wang, W.; et al. Calculating Structures and Free Energies of Complex Molecules: Combining Molecular Mechanics and Continuum Models. *Acc. Chem. Res.* **2000**, *33*, 889–897.
- (68) Massova, I.; Kollman, P. A. Combined Molecular Mechanical and Continuum Solvent Approach (MM-PBSA/GBSA) to Predict Ligand Binding. *Perspect. Drug Discov. Des.* **2000**, *18*, 113–135.
- (69) Connolly, M. L. Analytical Molecular Surface Calculation. *J. Appl. Crystallogr.* **1983**, *16*, 548–558.
- (70) Wang, J.; Wolf, R. M.; Caldwell, J. W.; Kollman, P. A.; Case, D. A. Development and Testing of a General Amber Force Field. *J. Comput. Chem.* **2004**, *25*, 1157–1174.
- (71) Jakalian, A.; Jack, D. B.; Bayly, C. I. Fast, Efficient Generation of High-quality Atomic Charges. AM1-BCC Model: II. Parameterization and Validation. *J. Comput. Chem.* **2002**, *23*, 1623–1641.
- (72) Onufriev, A.; Bashford, D.; Case, D. A. Exploring Protein Native States and Large-scale Conformational Changes with a Modified Generalized Born Model. *Proteins* **2004**, *55*, 383–394.
- (73) Rocha, G. B.; Freire, R. O.; Simas, A. M.; Stewart, J. J. P. RM1: a Reparameterization of AM1 for H, C, N, O, P, S, F, Cl, Br, and I. *J. Comput. Chem.* **2006**, *27*, 1101–1111.
- (74) Weis, A.; Katebzadeh, K.; Söderhjelm, P.; Nilsson, I.; Ryde, U. Ligand Affinities Predicted with the MM/PBSA Method: Dependence on the Simulation Method and the Force Field. *J. Med. Chem.* **2006**, *49*, 6596–6606.
- (75) Brown, S. P.; Muchmore, S. W. Rapid Estimation of Relative Protein-ligand Binding Affinities Using a High-throughput Version of MM-PBSA. *J. Chem. Inf. Model.* **2007**, *47*, 1493–1503.
- (76) Köhler, J.; Erlenkamp, G.; Eberlin, A.; Rumpf, T.; Slyko, I.; Metzger, E.; Schüle, R.; Sippl, W.; Jung, M. Lestaurtinib Inhibits Histone Phosphorylation and Androgen-dependent Gene Expression in Prostate Cancer Cells. *Plos One* **2012**, *7*, e34973.
- (77) Degliesposti, G.; Portoli, C.; Parenti, M. D.; Rastelli, G. BEAR, a Novel Virtual Screening Methodology for Drug Discovery. *J. Biomol. Screen.* **2011**, *16*, 129–133.
- (78) Graves, A. P.; Shivakumar, D. M.; Boyce, S. E.; Jacobson, M. P.; Case, D. A.; Shoichet, B. K. Rescoring Docking Hit Lists for Model Cavity Sites: Predictions and Experimental Testing. *J. Mol. Biol.* **2008**, *377*, 914–934.
- (79) Molecular Operating Environment (MOE); 2012.10; Chemical Computing Group Inc.: Montreal, QC, Canada, 2012.
- (80) Pickett, S. D.; Sternberg, M. J. Empirical Scale of Side-chain Conformational Entropy in Protein Folding. *J. Mol. Biol.* **1993**, *231*, 825–839.
- (81) Luo, R.; Gilson, M. K. Synthetic Adenine Receptors: Direct Calculation of Binding Affinity and Entropy. *J. Am. Chem. Soc.* **2000**, *122*, 2934–2937.
- (82) Golbraikh, A.; Tropsha, A. Beware of Q2! *J. Mol. Graph. Model.* **2002**, *20*, 269–276.
- (83) Golbraikh, A.; Tropsha, A. Predictive QSAR Modeling Based on Diversity Sampling of Experimental Datasets for the Training and Test Set Selection. *J. Comput. Aided Mol. Des.* **2002**, *16*, 357–369.
- (84) Golbraikh, A.; Shen, M.; Xiao, Z.; Xiao, Y.-D.; Lee, K.-H.; Tropsha, A. Rational Selection of Training and Test Sets for the Development of Validated QSAR Models. *J. Comput. Aided Mol. Des.* **2003**, *17*, 241–253.